and the Centre National de la Recherche Scientifique to J.C.C. is very gratefully acknowledged.

Registry No. $(CH_3)_3P\cdot GaCl_3$, 19502-93-3; $(C_2H_5)_3P\cdot GaCl_3$, 59400-56-5; $(CH_3)_2O\cdot GaCl_3$, 19379-37-4; $(CH_3)_2S\cdot GaCl_3$, 15171-34-3; $(CH_3)_3As\cdot GaCl_3$, 59400-54-3; $(CH_3)_3N\cdot GaCl_3$, 15555-33-6; $GaCl_3$, 13450-90-3.

Supplementary Material Available: A listing of structure factor amplitudes at two temperatures (12 pages). Ordering information is given on any current masthead page.

References and Notes

(1) J. C. Carter, R. Haran, and G. Jugie, *C. R. Hebd Seances Acad. Sci., Ser. C*, **282**, 623 (1976).
(2) P. H. Clippard, J. C. Hanson, and R. C. Taylor, *J. Cryst. Mol. Struct.*, **1**, 363 (1971).
(3) D. L. Black and R. C. Taylor, *Acta Crystallogr., Sect. B*, **31**, 1116 (1975).
(4) D. F. Grant and R. C. G. Killean, *Acta Crystallogr., Sect. B*, **25**, 377 (1969).
(5) M. Hargittai, I. Hargittai, and V. P. Spiridonov, *J. Mol. Struct.*, **30**, 31 (1976).
(6) D. F. R. Gilson and R. M. Hart, *Can. J. Chem.*, **48**, 1976 (1970).
(7) (a) W. Davies and W. Jones, *J. Chem. Soc.*, **132**, 1262 (1929); (b) E. G. Claeys, *J. Organomet. Chem.*, **5**, 446 (1966).
(8) Private communication with J. A. S. Smith.
(9) H. G. Fitzky, "Advances in Nuclear Quadrupole Resonance", Vol. 1, J. A. S. Smith, Ed., Heyden and Son, London, 1974, p 79.
(10) J. A. S. Smith and D. A. Tong, *J. Chem. Soc. A*, 178 (1971).
(11) D. T. Cromer and J. T. Waber, *Acta Crystallogr.*, **18**, 104 (1965).
(12) R. F. Stewart, E. R. Davidson, and W. T. Simpson, *J. Chem. Phys.*, **42**, 17 (1965).
(13) D. T. Cromer, *Acta Crystallogr.*, **18**, 17 (1965).
(14) W. Pies and A. Weiss, *J. Mol. Struct.*, **35**, 223 (1976).
(15) This program is part of a library package available from the Health Sciences Computing Facility of the University of California, Los Angeles, Calif. 90024.
(16) H. Bayer, *Z. Phys.*, **130**, 227 (1951).
(17) T. Kushida, G. B. Benedek, and N. Bloembergen, *Phys. Rev.*, **104**, 1364 (1956).
(18) R. J. C. Brown, *J. Chem. Phys.*, **32**, 116 (1960).
(19) J. M. Wenlersse, J. Virlet, and L. Guibe, *J. Chem. Phys.*, **63**, 5201 (1975).
(20) R. Chandramani, N. Devaraj, V. S. S. Sastry, and J. Ramakrishna, *Aust. J. Chem.*, **29**, 2363 (1976).
(21) L. M. Golubinskaya, A. V. Golubinskii, V. S. Mastryukov, L. V. Vilkov, and V. I. Bregadze, *J. Organomet. Chem.*, **117**, C4 (1976).
(22) R. Haran, J. P. Laurent, and G. Commenges, *Org. Magn. Reson.*, **5**, 463 (1973).
(23) T. Deeg and A. Weiss, *Ber. Bunsenges Phys. Chem.*, **79**, 497 (1975).
(24) D. A. Tong, *Chem. Commun.*, 790 (1969).
(25) (a) C. H. Townes and B. P. Dailey, *J. Chem. Phys.*, **17**, 782 (1949); **20**, 35 (1952); (b) E. A. C. Lucken, "Nuclear Quadrupole Coupling Constants", Academic Press, New York, N.Y., 1970, Chapter 7.
(26) S. C. Wallwork and I. J. Worral, *J. Chem. Soc.*, 1816 (1965).
(27) P. S. Bryan and R. L. Kuczkowski, *J. Chem. Phys.*, **55**, 3049 (1971).
(28) P. S. Bryan and R. L. Kuczkowski, *Inorg. Chem.*, **11**, 553 (1972).
(29) (a) W. A. G. Graham and F. G. A. Stone, *J. Inorg. Nucl. Chem.*, **3**, 164 (1956); (b) J. Demuynck and A. Veillard, *J. Chem. Soc. D*, 873 (1970); (c) I. H. Hillier and V. R. Saunders, *J. Chem. Soc. A*, 664 (1971).
(30) A. Balls, N. N. Greenwood, and B. P. Straughan, *J. Chem. Soc. A*, 753 (1968).

Contribution from the Institut für Physikalische und Theoretische Chemie, Universität Tübingen, Tübingen, West Germany, and Lehrstuhl B für Anorganische Chemie, Technische Universität Braunschweig, Braunschweig, West Germany

Molecular Structures of Phosphorus Compounds. 6. An Electron Diffraction Study of *tert*-Butylfluorophosphines $\mathrm{Bu}^t{}_n\mathrm{PF}_{3-n}$ (n = 1, 2, 3)

HEINZ OBERHAMMER,* REINHARD SCHMUTZLER, and OTHMAR STELZER

Received August 1, 1977

The geometric structures of *tert*-butyldifluorophosphine, di-*tert*-butylfluorophosphine, and tri-*tert*-butylphosphine have been determined in the gas phase by electron diffraction. Successive substitution of fluorine atoms by *tert*-butyl groups results in the lengthening of both P–F and P–C bond distances. The P–F bond lengths increase from 1.589 (3) Å in $\mathrm{Bu}^t\mathrm{PF}_2$ to 1.619 (7) Å in $\mathrm{Bu}^t{}_2\mathrm{PF}$. The P–C bond lengths increase even more strongly from 1.822 (12) Å in $\mathrm{Bu}^t\mathrm{PF}_2$ to 1.859 (6) Å in $\mathrm{Bu}^t{}_2\mathrm{PF}$ to 1.919 (5) Å in $\mathrm{Bu}^t{}_3\mathrm{P}$. The bond angles at the phosphorus atom follow the opposite trend. The CPF angle decreases from 99.0 (0.6)° in $\mathrm{Bu}^t\mathrm{PF}_2$ to 96.0 (2.0)° in $\mathrm{Bu}^t{}_2\mathrm{PF}$, and the CPC angle decreases from 113.8 (1.9)° in $\mathrm{Bu}^t{}_2\mathrm{PF}$ to 109.9 (0.7)° in $\mathrm{Bu}^t{}_3\mathrm{P}$. The geometric parameters and the configuration of the *tert*-butyl groups are given in the paper. The electron diffraction results are compared with results obtained by CNDO/2 calculations. The effect of steric strain on the geometry caused by the bulky *tert*-butyl groups is discussed.

Introduction

The phosphorus(III) ligands $\mathrm{Bu}^t{}_3\mathrm{P}$, $\mathrm{Bu}^t{}_2\mathrm{PF}$, and $\mathrm{Bu}^t\mathrm{PF}_2$ together with PF_3 constitute a complete substitution series, $\mathrm{Bu}^t{}_{3-n}\mathrm{PF}_n$ (n = 0–3).

The coordination chemistry of $\mathrm{Bu}^t\mathrm{PF}_2$,[1] $\mathrm{Bu}^t{}_2\mathrm{PF}$,[1,2] and $\mathrm{Bu}^t{}_3\mathrm{P}$[1,3,4] has been extensively studied, while the same is true even more for PF_3.[5a]

The coordination compounds synthesized range from transition-metal carbonyl complexes[1,3,5a] and transition-metal halide complexes, e.g., $\mathrm{MX}_2(\mathrm{Bu}^t{}_2\mathrm{PF})_2$ (M = Co, Ni; X = Cl, Br, I)[2] and $[\mathrm{Bu}^t{}_3\mathrm{PH}][\mathrm{NiBr}_3\mathrm{Bu}^t{}_3\mathrm{P}]$,[4a] to borane adducts, $\mathrm{Bu}^t{}_{3-n}\mathrm{PF}_n\cdot\mathrm{BH}_3$ (n = 0–3).[5b] The physical properties of these complexes have been thoroughly investigated.

The NMR spectroscopic properties of members of the series initially mentioned have been discussed in some detail,[1,6] and the Raman and infrared spectra of $\mathrm{Bu}^t\mathrm{PF}_2$[7] and $\mathrm{Bu}^t{}_2\mathrm{PF}$[8] have been assigned and interpreted.

UV photoelectron spectra[9] of these ligands show a remarkable decrease of the first vertical ionization potential from 12.3 eV (PF_3) to 7.70 eV ($\mathrm{Bu}^t{}_3\mathrm{P}$).

Finally, CNDO/2 calculations[10] of the differences in electronic energies of the phosphines $\mathrm{Bu}^t{}_{3-n}\mathrm{PF}_n$ and the corresponding phosphonium salts $[\mathrm{Bu}^t{}_{3-n}\mathrm{PF}_n\mathrm{H}]^+$ may be linearly related to the first vertical ionization potentials of the ligand $\mathrm{Bu}^t{}_{3-n}\mathrm{PF}_n$.

In order to show to what extent these observations could be explained on the basis of structural parameters of the phosphines $\mathrm{Bu}^t{}_{3-n}\mathrm{PF}_n$ (n = 0, 1, 2), a comparative electron diffraction study was undertaken.

Experimental Section

The phosphorus(III) compounds $\mathrm{Bu}^t\mathrm{PF}_2$,[11] $\mathrm{Bu}^t{}_2\mathrm{PF}$,[12] and $\mathrm{Bu}^t{}_3\mathrm{P}$[13,14] have been prepared according to the methods described in the literature. Their purity was checked by ^{1}H NMR, ^{19}F NMR, and ^{31}P NMR spectroscopy, respectively. The scattering intensities were recorded with the Balzers Diffractograph KD-G2[15] for two camera distances (25 and 50 cm) on Ilford N50 plates (18 × 13 cm). Details of the experiment are given in Table I. (Throughout this paper 1 Å = 100 pm and 1 Torr = 101.325/760 kPa.) The electron wavelength was determined by ZnO powder diffraction. For all molecules the s range ($s = (4\pi/\lambda)\sin(\delta/2)$, λ electron wavelength, δ scattering angle) covered in the experiment was s = 1.4–17 Å^{-1} and s = 7–34 Å^{-1} for the two camera distances. Two plates for each camera distance were selected for the structure analysis. The optical densities were

---

* To whom correspondence should be addressed at the Institut für Physikalische und Theoretische Chemie, Universität Tübingen.

Table I. Details of the Experiment

	Camera dist, cm	T_{sample}, °C	T_{nozzle}, °C	P_{camera}, 10^{-6} Torr	Exposure time, min	Electron wavelength, Å
Bu^tPF_2	50	−30	15	5	0.7–1.5	0.04925 (1)
	25	−26	15	15	2.5–3.5	0.04925 (2)
Bu^t_2PF	50	25	35	5	0.8–1.5	0.04928 (1)
	25	30	35	10	2.0–3.5	0.04925 (1)
Bu^t_3P	50	90	100	10	0.7–1.5	0.04918 (1)
	25	95	100	15	2.5–5.0	0.04915 (1)

measured with a modified Kipp + Zonen microdensitometer. The plate is rotated slowly and the transmission is recorded by an integrating voltmeter over a rotational angle of about 120°, since the plate is rectangular. After every revolution the plate is moved by 0.1 mm. For one plate about 700 points are recorded, which are then reduced to 78 and 135 data points, respectively, by interpolating the density data in steps of $\Delta s = 0.2$ Å^{-1}. The intensities I_i were obtained from the densities D_i by $I_i = D_i(1 + 0.07D_i)$. The intensities were divided by the sector function as determined from argon diffraction and multiplied by s^3. The preliminary background was refined for each plate separately by a procedure described elsewhere.[16] The averaged molecular intensities $sM^{\text{exptl}}(s)$ and the theoretical intensity functions for the final molecular models are shown in Figures 1, 4, and 7. Scattering amplitudes and phase shifts of Haase[17] were used.

Structure Determination

The radial distribution functions (Figures 2, 5, and 8) were used to obtain preliminary molecular models (Figures 3, 6, and 9). In the scattering range $0 < s < 1.4$ Å^{-1} the theoretical intensity functions were used in the Fourier transformation. The preliminary structural parameters and mean-square amplitudes were refined in a least-squares procedure based on the molecular intensities. The diagonal-weight matrix increases exponentially for $1.4 < s < 4$ Å^{-1}, remains one in the range $4 \leq s \leq 28$ Å^{-1}, and decreases exponentially for $28 < s < 34$ Å^{-1}. An interval of $\Delta s = 0.2$ Å^{-1} was chosen.

C_{3v} symmetry of the methyl and *tert*-butyl groups was assumed for all *tert*-butylfluorophosphines. There are two possible configurations for a *tert*-butyl group possessing C_{3v} symmetry, depending on whether all hydrogen atoms stagger or eclipse the bonds around the central carbon atom. In the staggered configuration the *tert*-butyl group "stands on three legs" on a plane perpendicular to the C_3 axis, while it "stands on six legs" in the eclipsed configuration. Both configurations were considered in the structure determinations. In all cases the staggered configuration was found experimentally.

For the estimation of error limits several effects have to be considered: (1) error in the s scale, (2) geometric constraints, (3) assumptions for mean-square amplitudes, (4) assumption of a "rigid" molecular model, and (5) correlation between experimental measurements. For the error in the s scale an upper limit of 0.1% is estimated. The effect of geometric constraints on the geometric parameters was investigated for tri-*tert*-butylmethane.[20] It was demonstrated that bond angles may be affected considerably, while bond distances are almost independent of such constraints. For the phosphines these effects will certainly be smaller than for the methane, since steric interactions between the *tert*-butyl groups are smaller. The neglect of large-amplitude torsional motion of the *tert*-butyl groups around the P–C bonds will affect strongly the torsional angle τ, which has to be interpreted as an effective angle and may deviate considerably from the equilibrium value. Since effects 2, 3, and 4 are very difficult to estimate, all standard deviations obtained from the least-squares analyses are multiplied by 3 to obtain error limits. This factor will also take account of effect 5. For bond distances the error in the s scale is considered separately.

Table II. Results for *tert*-Butyldifluorophosphine (r_a Structure)[a]

(a) Independent Geometric Parameters and Mean-Square Amplitudes					
P–F	1.589 (4)	0.044 (6)	C_t–C_1	1.517 (10)	0.050[b]
P–C_t	1.822 (12)	0.050 (10)	C–H	1.112 (11)	0.073 (10)
∠FPF	99.1 (1.7)		∠$C_1C_tC_2$	109.2 (1.3)	
∠C_tPF	99.0 (0.6)		∠HCH	108.5[b]	
(b) Scale Factors					
R_{50}	0.96 ± 0.04		R_{25}	0.91 ± 0.10	
(c) Dependent Geometric Parameters and Mean-Square Amplitudes					
P···C_1	2.74 (2)	0.173 (58)	F_1···C_1	2.89 (4)	0.091 (20)
F···C_t	2.60 (2)	0.063 (34)	F_1···C_2	3.10 (3)	
F_1···F_2	2.42 (3)	0.112 (19)	F_1···C_3	3.95 (2)	0.065 (25)
C_1···C_2	2.47 (3)				

[a] For numbering of atoms see Figure 3. Distance and mean-square amplitude in angstroms; angles in degrees. [b] Assumed.

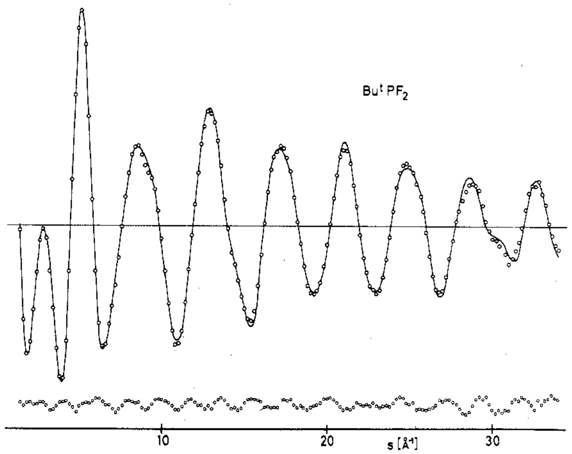

Figure 1. Bu^tPF_2 modified molecular intensities $sM^{\text{exptl}}(s)$ (OOO) and $sM^{\text{theor}}(s)$ (—) and differences.

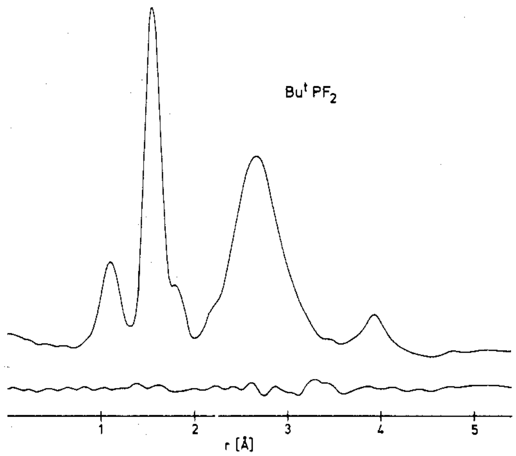

Figure 2. Bu^tPF_2 experimental radial distribution function and difference curve.

tert-**Butyldifluorophosphine,** $\mathbf{Bu^tPF_2}$. C_s symmetry was assumed for this molecule, the *tert*-butyl group staggering the PF_2 group. Furthermore, the HCH angle of methyl groups was fixed at a value of 108.5°. With these assumptions, four bond lengths and three bond angles have to be determined to describe the geometry of the molecule. In addition to these seven geometric parameters, eight mean-square amplitudes and the scale factors for the two camera distances, i.e., 17 parameters, were refined simultaneously in a least-squares procedure. Assumptions concerning the mean-square amplitudes can be seen in Table II. The following five correlation coefficients had values larger than 0.6: r(P–F)–r(C–C), 0.71; r(P–F)–∠CCC, 0.66; r(P–C)–∠CCC, 0.79; r(C–C)–∠CCC, 0.82; r(P–C)–l(P···C_1), 0.64. The results of the least-squares refinement are listed in Table II. The mean-square amplitudes involving hydrogen atoms were fixed at reasonable values.

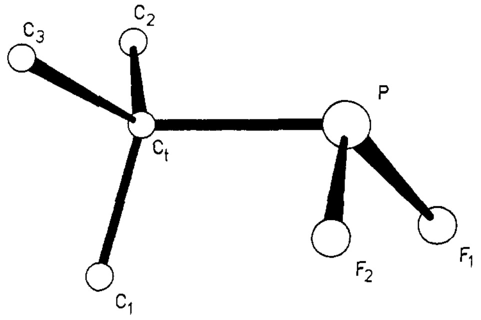

Figure 3. Bu^tPF_2 molecular model.

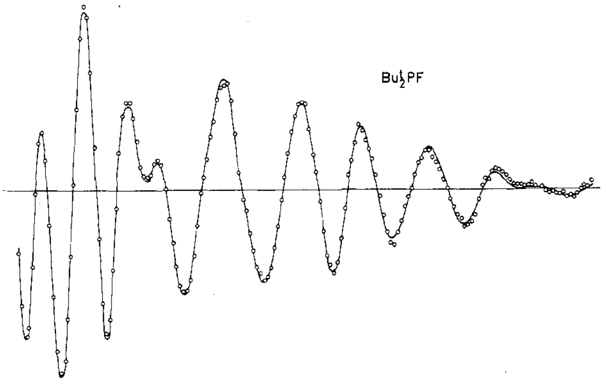

Figure 4. Bu^t_2PF modified molecular intensities $sM^{\text{exptl}}(s)$ (OOO) and $sM^{\text{theor}}(s)$ (—) and differences.

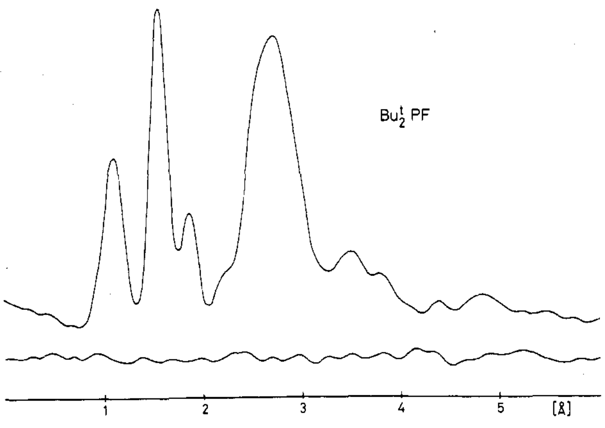

Figure 5. Bu^t_2PF experimental radial distribution function and difference curve.

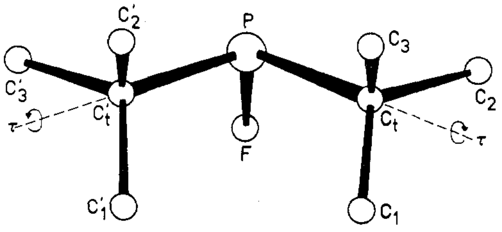

Figure 6. Bu^t_2PF molecular model.

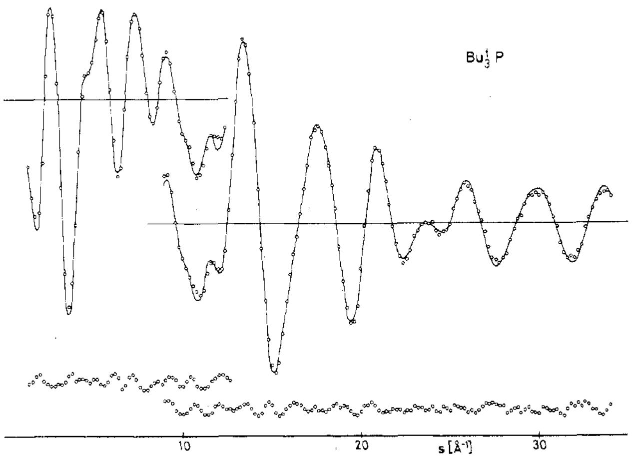

Figure 7. Bu^t_3P modified molecular intensities $sM^{\text{exptl}}(s)$ (OOO) and $sM^{\text{theor}}(s)$ (—) and differences.

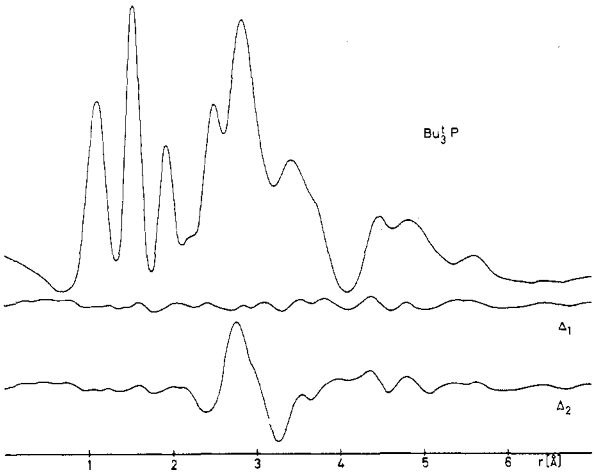

Figure 8. Bu^t_3P experimental radial distribution function, Δ_1 difference curve for staggered *tert*-butyl groups, and Δ_2 difference curve for eclipsed *tert*-butyl groups.

Di-*tert*-butylfluorophosphine, Bu^t_2PF. The overall symmetry of this molecule depends on the relative orientation of the two *tert*-butyl groups. If both groups are twisted around the P–C bonds in opposite directions, the symmetry will be C_s; the molecule possesses only C_1 symmetry if the *tert*-butyl groups are twisted in the same direction. Starting from a configuration with carbon atoms C_1 and C_3 (see Figure 6) staggering exactly the P–C_t bond (this corresponds to the twist angle $\tau = 0°$), the two possibilities of twisting were investigated. The radial distribution function is not very sensitive to the direction of twisting (C_1 or C_s symmetry) as long as $\tau < 10°$. Thus, both possibilities were considered in the least-squares procedure. After five geometric parameters and ten mean-square amplitudes were refined simultaneously, the sums of the errors squared obtained in the least-squares procedure were $\sigma(C_s) = 0.13$ and $\sigma(C_1) = 0.18$.

Although the experimental molecular intensities can be reproduced slightly better with a C_s model, the C_1 model cannot be ruled out definitely by the electron diffraction experiment. The twist angles obtained are $\tau(C_s) = 7.8 \pm 3.1°$ and $\tau(C_1) = 5.7 \pm 2.8°$, respectively. Figure 6 indicates the direction of the twist for the C_s model. All geometric parameters derived for the two models agree with each other within the error limits. Five correlation coefficients had values larger than 0.6: r(P–F)–l(C_t–C_1), 0.77; ∠CPC–l(F···C_t), 0.62; ∠HCH–l(P···C_1), 0.61; l(P···C_1)–l(F···C_t), 0.74; l(F···C_t)–l(C_1···C_2), 0.72. Table III lists the results of the least-squares refinement for the C_s model. In addition to the parameters given in Table III, the mean-square amplitude for the P···H distances was refined. A value of l(P···H) = 0.174 (46) Å was obtained. The other mean-square amplitudes involving hydrogen atoms were again fixed at reasonable values.

Tri-*tert*-butylphosphine, Bu^t_3P. Three bond lengths, three bond angles, and one twist angle determine the structure of this molecule when C_3 overall symmetry is assumed. Possible deviations of the *tert*-butyl groups from C_{3v} symmetry vs. C_3 symmetry were investigated for this molecule. A twist angle τ_m around the C_t–C bonds of all methyl groups was introduced as an additional parameter. Such a twist could reduce steric interactions between hydrogen atoms belonging to different *tert*-butyl groups. With starting values of $\tau_m = \pm 15°$ the least-squares procedure converged to $\tau_m = 3.7 \pm 6.5°$ and $\tau_m = -2.8 \pm 6.5°$, respectively. In both cases the sum of the errors

Table III. Results for di-*tert*-butylfluorophosphine (r_a structure)[a]

(a) Independent Geometric Parameters and Mean-Square Amplitudes

P–F	1.619 (7)	0.045[b]	C_t–C_1	1.530 (4)	0.051 (4)
P–C_t	1.859 (6)	0.057 (4)	C–H	1.107 (6)	0.084 (7)

∠C_tPF	96.0 (2.0)	∠C_tPC_t	113.8 (1.9)
∠$C_1C_tC_2$	109.6 (1.3)	∠HCH	108.1 (1.5)
τ	7.8 (3.1)		

(b) Scale Factors

R_{50}	0.88 ± 0.04	R_{25}	0.84 ± 0.07

(c) Dependent Geometric Parameters and Mean-Square Amplitudes

$C_1\cdots C_2$	2.50 (4)	0.088 (8)	$C_t\cdots C_1'$	3.58 (8)	0.111 (43)
$F\cdots C_t$	2.59 (4)	0.122 (114)	$C_t\cdots C_2'$	3.42 (9)	
$P\cdots C_1$	2.77 (4)	0.148 (42)	$C_t\cdots C_3'$	4.42 (4)	
$F\cdots C_1$	2.67 (10)	0.155 (43)	$C_1\cdots C_1'$	3.37 (15)	0.184 (83)
$F\cdots C_2$	3.31 (5)		$C_1\cdots C_2'$	4.04 (9)	
$F\cdots C_3$	3.90 (6)		$C_1\cdots C_3'$	4.99 (9)	
$C_t\cdots C_t'$	3.12 (5)	0.120[b]	$C_2\cdots C_2'$	4.78 (10)	
			$C_2\cdots C_3'$	5.53 (8)	
			$C_3\cdots C_2'$	3.00 (16)	

[a] For numbering of atoms see Figure 6. Distances and mean-square amplitudes in angstroms; angles in degrees. [b] Assumed.

Table IV. Results for Tri-*tert*-butylphosphine (r_a Structure)[a]

(a) Independent Geometric Parameters and Mean-Square Amplitudes

P–C_t	1.919 (5)	0.060 (5)
C_t–C_1	1.534 (3)	0.055 (4)
C–H	1.106 (5)	0.090 (7)

∠C_tPC_t'	109.9 (0.7)	∠$C_1C_tC_2$	107.8 (0.4)
∠HCH	107.2 (1.2)	τ	14.0 (1.3)

(b) Scale Factors

R_{50}	0.80 ± 0.04	R_{25}	0.78 ± 0.08

(c) Dependent Geometric Parameters and Mean-Square Amplitudes

$C_1\cdots C_2$	2.48 (1)	0.068 (5)	$C_1\cdots C_1'$	3.32 (5)	0.257 (67)
$P\cdots C_1$	2.86 (1)	0.142 (10)	$C_1\cdots C_3'$	3.56 (5)	
$C_t\cdots C_t'$	3.14 (2)	0.120[b]	$C_2\cdots C_3'$	3.29 (2)	
$C_t\cdots C_1'$	3.70 (3)	0.107 (15)	$C_1\cdots C_2'$	4.90 (3)	0.188 (36)
$C_t\cdots C_3'$	3.38 (2)		$C_2\cdots C_1'$	4.52 (4)	
$C_t\cdots C_1''$	3.39 (3)		$C_3\cdots C_1'$	4.96 (3)	
$C_t\cdots C_2''$	3.69 (2)		$C_2\cdots C_2'$	4.94 (2)	
$C_t\cdots C_2'$	4.48 (1)	0.123 (25)	$C_3\cdots C_2'$	5.68 (2)	
$C_t\cdots C_3''$	4.48 (2)		$C_3\cdots C_3'$	4.89 (2)	

[a] For numbering of atoms see Figure 9. Distances and mean-square amplitudes in angstroms; angles in degrees. [b] Assumed.

squared decreased by less than 10%. Thus, C_{3v} symmetry for the *tert*-butyl groups ($\tau_m = 0°$) was assumed in the further calculations.

Nine mean-square amplitudes were refined simultaneously with the seven geometric parameters. Only two correlation coefficients had values larger than 0.6: ∠HCH–∠CCC, 0.66; ∠HCH–$l(P\cdots C_1)$, 0.68. The final results are listed in Table IV. For the P···H mean-square amplitude a value of $l(P\cdots H) = 0.239$ (48) Å was derived. For $Bu^t{}_3P$ the effect of the configuration of the *tert*-butyl groups on the radial distribution function is demonstrated in Figure 8. The difference curve Δ_1 corresponds to the configuration with all hydrogen atoms staggering the bonds around the C_t atom, while Δ_2 corresponds to the eclipsed configuration.

Discussion

Molecular orbital calculations in the CNDO/2 approximation have been performed for di-*tert*-butylfluorophosphine[18] and tri-*tert*-butylphosphine.[19] In both cases the optimized CPC bond angles agree very well with the experimental results (114.5 and 108.2°, respectively). All other geometric parameters and the results concerning the configuration of the *tert*-butyl groups, however, are in disagreement with the electron diffraction results. For $Bu^t{}_2PF$ the optimized P–C and C–C distances (1.836 and 1.476 Å) are too short, while the angles FPC (106.1°) and CCC (114.5°) are larger than the experimental values by 10 and 5°, respectively. Moreover, the configuration of the *tert*-butyl groups is predicted to be eclipsed with a twist angle $\tau = 24°$, while the electron diffraction experiment results in a staggered configuration with $\tau = 7.8$ (3.1)°. The problem of the overall symmetry of the molecule (C_s or C_1) has not been investigated with the CNDO/2 method. C_s symmetry was assumed in the MO calculations. For $Bu^t{}_3P$ the P–C and C–C bond lengths were assumed to be 1.846 and 1.548 Å. The optimized CCC angle (112.1°) is about 4° larger than the electron diffraction value. The small experimental value for the CCC angle in $Bu^t{}_3P$ of 107.8 (0.4)° agrees with the corresponding value determined for tri-*tert*-butylmethane[20] (105.7 ± 0.2°), indicating that steric interactions between the three *tert*-butyl groups lead to a decrease of this angle. The short P–C bond assumed in the CNDO/2 calculations (0.07 Å shorter than the experimental value) may explain the good agreement between the optimized CPC angle and the experimental result (108.2 and 109.9 (0.7)°, respectively). The increased steric interaction due to the short bond is compensated in the MO calculations by opening the bond angles at the phosphorus atom. Using the experimental P–C bond length of about 1.92 Å in the CNDO/2 calculations would probably make the agreement between optimized and experimental CPC angles worse. For $Bu^t{}_3P$ the CNDO/2 calculations again predict eclipsed *tert*-butyl groups and an energy difference between eclipsed and staggered configurations of 154 kcal mol^{-1}. The electron diffraction intensities, however, can definitely not be fitted with eclipsed *tert*-butyl groups (see Figure 8). From this discrepancy we have to conclude that steric interactions between hydrogen atoms, which to a large extent determine the configuration of the *tert*-butyl groups, are not accounted for properly in the CNDO/2 approximation.

Table V summarizes the geometric parameters for the series $Bu^t{}_nPF_{3-n}$ with n = 0, 1, 2, and 3. The P–F and P–C bond lengths increase almost linearly with the increasing number

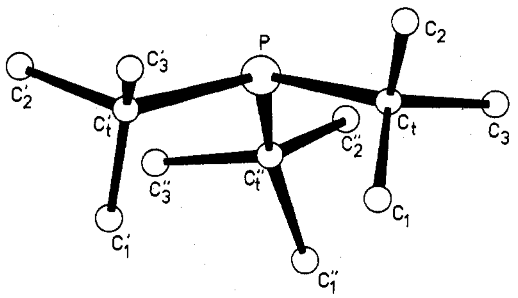

Figure 9. $Bu^t{}_3P$ molecular model.

Table V. Geometric Parameters for $Bu^t{}_nPF_{3-n}$, n = 0, 1, 2, 3 (r_a values)[a]

	PF_3[b]	Bu^tPF_2	$Bu^t{}_2PF$	$Bu^t{}_3P$
P–F	1.569 (1)	1.589 (4)	1.619 (7)	
P–C_t		1.822 (12)	1.859 (6)	1.919 (5)
C_t–C		1.517 (10)	1.530 (4)	1.534 (3)
C-H		1.112 (11)	1.107 (7)	1.106 (5)
∠FPF	97.7 (0.2)	99.1 (1.7)		
∠C_tPF		99.0 (0.6)	96.0 (2.0)	
∠C_tPC_t			113.8 (1.9)	109.9 (0.7)
∠CC_tC		109.2 (1.3)	109.6 (1.3)	107.8 (0.4)
∠HCH		108.5[c]	108.1 (1.5)	107.2 (1.2)
τ		0[c]	7.8 (3.1)	14.0 (1.3)
$F\cdots F$	2.36 (1)	2.42 (3)		
$F\cdots C_t$		2.60 (2)	2.59 (4)	
$C_t\cdots C_t$			3.12 (5)	3.14 (2)

[a] Distances in angstroms; angles in degrees. [b] Reference 23. [c] Assumed.

of *tert*-butyl groups, whereby the lengthening of the P–C bond is about twice as large as for the P–F bond. It should be pointed out that the variation of the P–C bond length from Bu^tPF_2 to Bu^t_3P is almost 0.1 Å. The bond angles at the central phosphorus atom do not show such an obvious correlation with the number of *tert*-butyl groups. The increase of the FPF angle from PF_3 to Bu^tPF_2 is only 1.4° and is within the error limits. The CPF and CPC angles, however, decrease by about 3 and 4°, respectively when one fluorine atom is substituted by a *tert*-butyl group. From crude steric considerations the opposite trend would be expected. The nonbonded $F\cdots C_t$ and $C_t\cdots C_t$ distances give a plausible explanation for the observed trend in the bond angles. Both distances are remarkably constant when the number of *tert*-butyl groups is increased. Thus, the large CPC angle in Bu^t_2PF can be understood on the basis of the P–C bond lengths and the $C_t\cdots C_t$ nonbonded distance. The F···F distances do not show this constant behavior.

The geometric parameters for Bu^t_2PF in the gas phase agree quite well with the corresponding values for the *trans*-dibromo(di-*tert*-butylfluorophosphine)nickel(II) complex in the crystal: P–C = 1.86 (1) and 1.88 (1) Å, P–F = 1.579 (7) Å, CPF = 97.3 (0.5) and 97.9 (0.5)°, and CPC = 113.8 (0.6)°. Only the P–F distances in the gas phase and in the crystal do not agree with each other.

The effect of steric strain on the geometry of a molecule can be demonstrated very clearly by comparing the structures of trimethylphosphine[21] and tri-*tert*-butylphosphine. The P–C bond lengths increase from 1.846 (3) to 1.919 (5) Å (Δr_{P-C} = 0.073 (6) Å). The same variation has been determined for the C–C bond length in isobutane[22] and tri-*tert*-butylmethane,[20] which increases from 1.535 (1) to 1.611 (5) Å (Δr_{C-C} = 0.076 (5) Å). However, the effect on the bond angles is much stronger in the phosphines, where an increase of 11.3 (0.8)° (from 98.6 (0.3) to 109.9 (0.7)°) is observed, whereas the difference is only 5.8 (0.5)° (110.9 (0.2)° for Me_3CH and 116.0 (0.4)° for Bu^t_3CH) for the methane derivatives. The CPC bond angles in tri-*tert*-butylphosphine indicate that the steric interactions between two *tert*-butyl groups are very similar to the steric interactions between a *tert*-butyl group and the lone electron pair.

Registry No. Bu^tPF_2, 29149-32-4; Bu^t_2PF, 29146-24-5; Bu^t_3P, 13716-12-6.

References and Notes

(1) O. Stelzer and R. Schmutzler, *J. Chem. Soc. A*, 2867 (1971).
(2) O. Stelzer and E. Unger, *J. Chem. Soc., Dalton Trans.*, 1783 (1973); W. S. Scheldrick and O. Stelzer, *ibid.*, 926 (1973).
(3) H. Schumann, O. Stelzer, and U. Niederreuther, *J. Organomet. Chem.*, **16**, P64 (1969).
(4) (a) E. C. Alyea, A. Costin, G. Ferguson, G. T. Fey, R. G. Goel, and R. J. Restivo, *J. Chem. Soc., Dalton Trans.*, 1294 (1975); (b) C. A. Tolman, *J. Am. Chem. Soc.*, **92**, 2953 (1970).
(5) (a) J. F. Nixon, *Adv. Inorg. Chem. Radiochem.*, **13**, 364 (1970); O. Stelzer, *Top. Phosphorus Chem.*, **9**, 1 (1977); (b) C. Jouany, C. Jugie, J. P. Laurent, R. Schmutzler, and O. Stelzer, *J. Chim. Phys. Phys.-Chim. Biol.*, **71**, 395 (1974).
(6) C. Schumann, H. Dreeskamp, and O. Stelzer, *Chem. Commun.*, 619 (1970).
(7) R. R. Holmes and M. Fild, *Spectrochim. Acta, Part A*, **27**, 1525 (1971).
(8) R. R. Holmes, G. Ting-kuo Fey, and R. H. Larkin, *Spectrochim. Acta, Part A*, **29**, 665 (1973).
(9) M. F. Lappert, J. B. Pedley, B. T. Wilkins, O. Stelzer, and E. Unger, *J. Chem. Soc., Dalton Trans.*, 1207 (1975).
(10) M. Graffeuil, J. F. Labarre, M. F. Lappert, C. Leibovici, and O. Stelzer, *J. Chim. Phys. Phys.-Chim. Biol.*, **71**, 395 (1974).
(11) M. Fild and R. Schmutzler, *J. Chem. Soc. A*, 2359 (1970).
(12) O. Stelzer and R. Schmutzler, *Inorg. Synth.*, in press.
(13) H. Hoffmann and P. Schellenbeck, *Chem. Ber.*, **100**, 692 (1967).
(14) L. Maier, *Org. Phosphorus Compd.*, **1**, 128 (1972).
(15) W. Zeil, J. Haase, and L. Wegmann, *Z. Instrumentenkd.*, **74**, 84 (1966).
(16) H. Oberhammer and S. H. Bauer, *J. Am. Chem. Soc.*, **91**, 10 (1969).
(17) J. Haase, *Z. Naturforsch., A*, **25**, 936 (1970).
(18) M. Corosine and F. Crasnier, *J. Mol. Struct.*, **27**, 105 (1975).
(19) M. Corosine, F. Crasnier, J. F. Labarre, J. M. Labarre, and C. Leibovici, *J. Mol. Struct.*, **22**, 257 (1974).
(20) H. B. Burgi and L. S. Bartell, *J. Am. Chem. Soc.*, **94**, 5239 (1972).
(21) L. S. Bartell, *J. Chem. Phys.*, **32**, 515 (1960).
(22) R. L. Hilderbrandt and J. D. Wieser, *J. Mol. Struct.*, **15**, 27 (1973).
(23) Y. Morino, K. Kuchitsu, and T. Moritani, *Inorg. Chem.*, **8**, 867 (1969).

Contribution from the Department of Chemistry,
Colorado State University, Fort Collins, Colorado 80523

Crystal and Molecular Structure of (Cyanato-*N*)[difluoro-3,3′-(trimethylenedinitrilo)bis(2-butanone oximato)borato]copper(II), Cu(cyclops)(NCO)

OREN P. ANDERSON* and J. C. MARSHALL

Received August 22, 1977

The crystal and molecular structure of Cu(cyclops)(NCO) (cyclops = difluoro-3,3′-(trimethylenedinitrilo)bis(2-butanone oximato)borate), $[Cu(C_{11}H_{18}N_4O_2BF_2)(NCO)]$, has been determined from three-dimensional single-crystal x-ray diffraction data, collected by counter techniques. The dark green crystals are monoclinic, space group $P2_1/c$ (No. 14), with four formula units in a unit cell of dimensions a = 13.552 (4) Å, b = 11.818 (4) Å, c = 11.634 (5) Å, and β = 113.69 (1)°. The structure was refined by full-matrix least-squares methods to an R value of 0.045 (R_w = 0.050) for 1528 independent reflections with $F^2 > 3\sigma(F^2)$. The coordination geometry about the copper(II) ion in the neutral monomeric complex is based on a square pyramid. While the Cu–N bonds to the macrocycle exhibit bond lengths in the normal range (1.990 (5)–2.009 (5) Å), the displacement of the copper(II) ion above the least-squares plane through these four nitrogen atoms is very large (0.58 Å). This extremely large axial displacement of the copper(II) ion is accompanied by formation of an unusually strong bond to the axial cyanato-*N* ligand, with the Cu–N1(cyanate) distance found to be 2.038 (6) Å. This very short axial bond is felt to be a consequence of the unique electronic and steric properties of this unusual uninegative macrocyclic ligand.

Introduction

Transition-metal complexes of the macrocyclic ligand difluoro-3,3′-(trimethylenedinitrilo)bis(2-butanone oximato)borate (**1**, R = CH_3, hereafter referred to as cyclops) and related ligands of the general formulation **1**, together with complexes of the precursor dioxime ligands of these macrocycles, have recently been the subjects of several chemical and structural studies.[1-6] The studies of the difluoro–borate

0020-1669/78/1317-1258$01.00/0 © 1978 American Chemical Society